npg

ORIGINAL ARTICLE

Stat3 regulates ErbB-2 expression and co-opts ErbB-2 nuclear function to induce miR-21 expression, PDCD4 downregulation and breast cancer metastasis

L Venturutti[1], LV Romero[1], AJ Urtreger[2], MF Chervo[1], RI Cordo Russo[1], MF Mercogliano[1], G Inurrigarro[3], MG Pereyra[1], CJ Proietti[1], F Izzo[1], MC Díaz Flaqué[1], V Sundblad[1], JC Roa[4,5,6], P Guzmán[4], ED Bal de Kier Joffé[2], EH Charreau[1], R Schillaci[1] and PV Elizalde[1]

Membrane overexpression of the receptor tyrosine kinase ErbB-2 (MErbB-2) accounts for a clinically aggressive breast cancer (BC) subtype (ErbB-2-positive) with increased incidence of metastases. We and others demonstrated that nuclear ErbB-2 (NErbB-2) also plays a key role in BC and is a poor prognostic factor in ErbB-2-positive tumors. The signal transducer and activator of transcription 3 (Stat3), another player in BC, has been recognized as a downstream mediator of MErbB-2 action in BC metastasis. Here, we revealed an unanticipated novel direction of the ErbB-2 and Stat3 interaction underlying BC metastasis. We found that Stat3 binds to its response elements (GAS) at the ErbB-2 promoter to upregulate ErbB-2 transcription in metastatic, ErbB-2-positive BC. We validated these results in several BC subtypes displaying metastatic and non-metastatic ability, highlighting Stat3 general role as upstream regulator of ErbB-2 expression in BC. Moreover, we showed that Stat3 co-opts NErbB-2 function by recruiting ErbB-2 as its coactivator at the GAS sites in the promoter of microRNA-21 (miR-21), a metastasis-promoting microRNA (miRNA). Using an ErbB-2 nuclear localization domain mutant and a constitutively activated ErbB-2 variant, we found that NErbB-2 role as a Stat3 coactivator and also its direct role as transcription factor upregulate miR-21 in BC. This reveals a novel function of NErbB-2 as a regulator of miRNAs expression. Increased levels of miR-21, in turn, downregulate the expression of the metastasis-suppressor protein programmed cell death 4 (PDCD4), a validated miR-21 target. Using an in vivo model of metastatic ErbB-2-postive BC, in which we silenced Stat3 and reconstituted ErbB-2 or miR-21 expression, we showed that both are downstream mediators of Stat3-driven metastasis. Supporting the clinical relevance of our results, we found an inverse correlation between ErbB-2/Stat3 nuclear co-expression and PDCD4 expression in ErbB-2-positive primary invasive BCs. Our findings identify Stat3 and NErbB-2 as novel therapeutic targets to inhibit ErbB-2-positive BC metastasis.

Oncogene advance online publication, 27 July 2015; doi:10.1038/onc.2015.281

INTRODUCTION

Metastasis is one of the hallmarks of breast cancer (BC) and the principal cause of death from this disease. Membrane overexpression of ErbB-2/HER-2 (MErbB-2), a member of the ErbBs family of receptor tyrosine kinases (RTKs: EGF-R/ErbB-1, ErbB-2, ErbB-3 and ErbB-4), underlies a clinically aggressive BC subtype (ErbB-2-positive) with high incidence of metastases.[1–3] Although an orphan receptor, upon ligand binding to the other ErbB family members, ErbB-2 forms heterodimers. In the absence of ligands, it also assembles homo and heterodimers in MErbB-2-overexpressing BC.[4,5] Dimerization stimulates ErbB-2 tyrosine (Tyr) kinase activity and results in the activation of signaling pathways, the canonical mechanism of ErbB-2 action. Accumulating evidence, including our own, showed that ErbB-2 also activates the signal transducer and activator of transcription 3 (Stat3) pathway, which acts as a downstream effector of ErbB-2-induced initiation and metastatic dissemination of BC.[6–9] Stat3 function as transcription factor (TF), along with the facts that it is by itself a critical player in BC growth and metastasis[10] and that it is constitutively activated

in invasive ErbB-2-positive BC[6,7,9,11] demand further study to better understand the nature of the ErbB-2/Stat3 interaction in BC. Intriguingly, Stat3 capacity to act as an upstream activator of ErbB-2 in metastatic BC remains unexplored.

Compelling findings, including ours, demonstrated that MErbB-2 migrates to the nucleus (nuclear ErbB-2 (NErbB-2)) of BC cells, where it binds promoters/enhancers of target genes.[12–17] We discovered that at the nucleus, ErbB-2 assembles a transcriptional complex in which it functions as a coactivator of Stat3 to upregulate cyclin D1 and p21[CIP1] expression, and to promote BC growth and resistance to anti-MErbB-2 therapies.[12–17] Therapeutic options for ErbB-2-positive BC target MErbB-2 with monoclonal antibodies and a drug-conjugated antibody, or block its Tyr kinase activity. Drugs targeting the ErbB-2 downstream phosphatidylinositol-3 kinase/Akt/mTOR pathway are currently being tested in clinical trials. However, there are no undergoing trials that target NErbB-2 or block upstream ErbB-2 activators. In this framework, where disease progression in the metastatic setting will inevitably follow the administration of current

2

therapies, we explored whether the Stat3/ErbB-2 interaction may be bidirectional, that is, Stat3 acts as an upstream activator of ErbB-2 in BC, and investigated whether the nuclear Stat3/ErbB-2 complex is involved in Stat3-regulated metastasis. We chose to examine the assembly of said complex at the promoter of microRNA-21 (miR-21), a microRNA (miRNA) aberrantly upregulated in a plethora of cancer types.[18–23] In particular, miR-21, whose expression is regulated by ErbB-2 and Stat3, has been identified as a key player at the stage of BC metastasis.[24–28] Indeed, it was reported that miR-21 forced expression in BC cells enhances their migration and invasion capacity.[29,30] Moreover, previous findings have found a direct correlation between miR-21 levels and the metastatic dissemination of human BC tumor samples.[31–33] Our findings revealed that Stat3 regulates ErbB-2 expression and co-opts its nuclear function to induce miR-21 and BC metastasis, highlighting Stat3 and NErbB-2 as novel targets to block metastatic dissemination in MErbB-2-positive BC.

RESULTS

Stat3 controls ErbB-2 transcription in BC

We first assessed whether Stat3 acts as an upstream regulator of ErbB-2 expression in ErbB-2-positive BC. We used metastatic LM3 murine BC cells overexpressing ErbB-2 (refs. 34, 35), and metastatic ErbB-2-amplified MDA-MB-453 human BC cells.[36] We already reported that ErbB-2 is constitutively Tyr phosphorylated in LM3 cells.[34] Previously, we showed that ErbB-2 is present at the membrane and the nucleus of MDA-MB-453 cells.[13] Here, we found that it is also constitutively phosphorylated at Tyr1222 residue in said cells (Supplementary Figure S1a). Under growth conditions, both lines show Stat3 phosphorylation levels at Tyr705 comparable to those in T47D BC cells stimulated with the synthetic progestin medroxiprogesterone acetate (MPA), previously considered as high (Figure 1a).[37] Silencing of ErbB-2 expression significantly reduced Stat3 phosphorylation in both lines (Supplementary Figure S1b shows results in MDA-MB-453 cells), showing that Stat3 is activated downstream of ErbB-2, as observed in several BC models.[6,9,11] We and others demonstrated that Stat3 Tyr705 phosphorylation is mandatory for its nuclear translocation and transcriptional activity.[37,38] Stat3 phosphorylation was significantly reduced upon transient transfection with the dominant negative (DN) Stat3Y705-F expression vector, which carries a Tyr-to-phenylalanine substitution that reduces Tyr705 phosphorylation of endogenous Stat3, thus inhibiting its transcriptional activity (Figure 1a).[37–39] We also obtained stable clones of LM3 cells expressing Stat3Y705-F (DN1 to DN3), which showed different inhibition degrees of Tyr705 phosphorylation compared with a clone generated with the empty vector (VECTOR) (Figure 1a). Interestingly, a significant reduction of ErbB-2 protein levels was found in DN clones as compared with those of the VECTOR clone (Figure 1b). Likewise, ErbB-2 protein was downregulated when we silenced Stat3 (Figure 1c). Stat3 knockdown also inhibited ErbB-2 expression in poorly metastatic MCF-7 BC cells displaying estrogen receptor (ER) and moderate amounts of MErbB-2 (surrogate of luminal A molecular subtype), in non-metastatic ER and PR-positive and ErbB-2-overexpressing BT-474 cells (surrogate of luminal B-like ErbB-2-positive tumors), in non-metastatic ER and PR-negative and ErbB-2-positive JIMT-1 BC cells (ErbB-2-positive subtype), and in metastatic triple-negative (ER, PR and MErbB-2-negative) MDA-MB-231 BC cells (Figure 1d).[40] Furthermore, Stat3 silencing significantly reduced ErbB-2 messenger RNA (mRNA) levels in cell lines from different BC molecular subtypes (Figure 1e). Next, we transfected LM3 cells with a luciferase reporter plasmid downstream of the human ErbB-2 promoter, which includes a Stat3 binding site (GAS).[41] Stat3 knockdown using a small interfering RNA (siRNA) significantly inhibited ErbB-2 promoter activation (Figure 1f). Chromatin

immunoprecipitation (ChIP) assays in MDA-MB-453 cells revealed that Stat3 is recruited to this GAS site (Figure 1g). CREB binding protein (CBP), a coactivator with histone acetyltransferase activity and marker of active gene transcription, was also recruited to the site (Figure 1g). Accordingly, analysis of the local chromatin architecture revealed high levels of histone H4 acetylation (H4Ac), a marker of chromatin activation. Inhibition of Stat3 activation by transfection with Stat3Y705-F successfully reduced Stat3 loading to the ErbB-2 promoter, inhibited CBP recruitment and significantly decreased H4Ac levels (Figure 1g). Our findings reveal a novel direction of the interaction between ErbB-2 and Stat3, where Stat3 induces ErbB-2 promoter transcriptional activation and expression in ErbB-2-positive metastatic BC. Furthermore, our results in several BC molecular subtypes, displaying both metastatic and non-metastatic ability, highlight Stat3 general role as an upstream regulator of ErbB-2 expression in BC.

Stat3 recruits ErbB-2 as its coactivator to upregulate miR-21 expression

We showed that a transcriptional complex in which activated ErbB-2 acts a Stat3 coactivator is assembled at the GAS sites of cyclin D1 and p21[CIP1] promoters.[12–15] Owing to miRNAs capacity to target multiple genes, we decided to study the assembly of said complex at the promoter of miRNAs. This approach will then allow us to investigate the complex role in the regulation of miRNA targets within gene networks involved in metastasis. We chose to examine miR-21, whose expression was found to be associated with enhanced BC metastasis.[42] In addition, Stat3 function as TF and ErbB-2 downstream-activated signaling pathways induce miR-21 expression in BC and other cancer cell types.[24–28] We found that Stat3 silencing decreased miR-21 in several metastatic and non-metastatic BC subtypes (Figure 2a). ErbB-2 silencing also reduced miR-21 expression in LM3, MDA-MB-453, JIMT-1 and BT-474 cells (Figure 2b). Immunofluorescence (IF) staining[12,13] detected nuclear ErbB-2 (NErbB-2) and Stat3 (NStat3) in LM3 and MDA-MB-453 cells, and their nuclear colocalization (Figure 2c). Indeed, quantitative analysis of confocal images revealed high levels of NErbB-2 and NStat3 in these cells (Figure 2c). To explore NErbB-2 action on miR-21 expression, we transfected cells with hErbB-2ΔNLS (Figure 2d), a human ErbB-2 nuclear localization domain mutant unable to translocate to the nucleus,[16] which functions as a DN inhibitor of endogenous ErbB-2 nuclear migration.[12,13] hErbB-2ΔNLS retains intrinsic Tyr kinase activity and the capacity to activate ErbB-2 cascades, including p42/p44 mitogen-activated protein kinase (MAPKs), and it does not affect endogenous ErbB-2 signaling.[12,13,16] hErbB-2ΔNLS transfection inhibited ErbB-2 nuclear localization in MDA-MB-453 (Figure 2d) and LM3 cells (not shown). Abrogation of NErbB-2 presence decreased miR-21 levels in both cell lines (Figure 2e). ChIP and sequential ChIP assays using primers flanking a GAS site at position − 1230 and spanning two sites at − 938 and − 907 (ref. 25), relative to human miR-21 transcriptional start site,[43] or using primers flanking a GAS site at − 3111 and spanning two sites at − 2810 and − 2779 (MatInspector (http://www.genomatix.de)) from the murine pre-miR-21, revealed that Stat3 and ErbB-2 are simultaneously recruited to the miR-21 promoter (Figures 2f and g). To gain insight into the mechanism of NErbB-2/NStat3 interaction we explored the chromatin activation state of the miR-21 promoter at GAS site 1 in MDA-MB-453 cells. CBP, a marker of active gene transcription, was recruited to said site. Consistently, high H4Ac levels were detected in MDA-MB-453 cells (Figure 2h). We then inhibited NErbB-2 presence by transfection with hErbB-2ΔNLS. As we reported,[12] hErbB-2ΔNLS did not affect Stat3 loading, but inhibited CBP recruitment and markedly decreased H4Ac levels. Our results reveal that a complex in which ErbB-2 acts as a coactivator of Stat3 induces miR-21 expression in
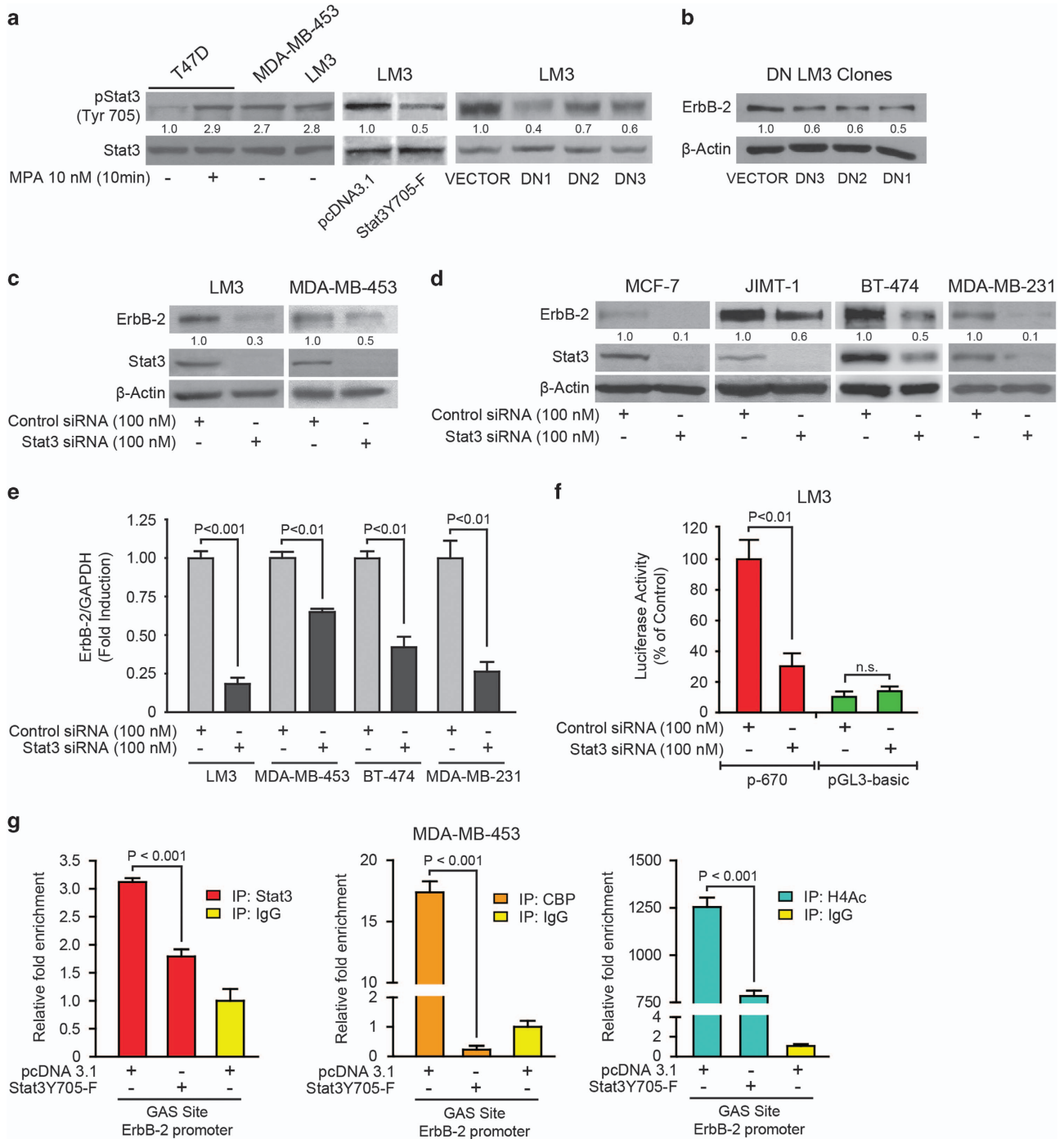
Figure 1. Stat3 controls ErbB-2 expression in BC cells. (**a**) T47D cells were treated with MPA or MDA-MB-453 and LM3 cells were serum-stimulated (left); LM3 cells were transiently transfected with Stat3Y705-F vector (middle) or were stably transfected with Stat3Y705-F (DN clones) or empty vector (VECTOR clone) (right). WB analyses were performed with a pStat3 antibody, and filters were reprobed with a total Stat3 antibody. (**b**) ErbB-2 levels were analyzed by WB. β-actin expression was used as loading control. (**c**, **d**) Cells were transfected with Stat3 or control siRNA and ErbB-2 expression was analyzed by WB. Experiments shown in (**a**–**d**) are representative of a total of three, with similar results. Numbers under each blot represent the corresponding densitometric quantification. (**e**) Cells were transfected as indicated and ErbB-2 mRNA levels were measured by RT-qPCR. Fold change of mRNA levels was calculated by normalizing the absolute levels of ErbB-2 mRNA to those of GAPDH, used as an internal control, setting the value of control siRNA-transfected cells to 1. (**f**) Stat3 controls ErbB-2 expression at the transcriptional level. Cells were co-transfected with Stat3 or control siRNA and a human ErbB-2 promoter luciferase construct (p-670-Luc), which contains a Stat3 binding site, or the empty plasmid. *Renilla* luciferase was used for normalization. Results are presented as percentage of inhibition, setting the value of control siRNA-transfected cells to 100%. (**g**) Stat3 is recruited to the ErbB-2 promoter. Cells were transfected with Stat3Y705-F and recruitment of Stat3 and CBP, and acetyl-histone H4 (H4Ac) levels at the ErbB-2 promoter were analyzed by ChIP. Immunoprecipitated DNA was amplified by RT-qPCR using primers flanking the GAS site at position − 529. Amounts immunoprecipitated for each sample are reported relative to the amount obtained for IgG, used as a negative control, which was set to 1. Data shown in (**e**–**g**) represent the mean ± s.e.m of three independent experiments. See Supplementary Figure S1.

metastatic BC. Moreover, this is the first report on NErbB-2 ability to upregulate a miRNA in any normal or malignant cell type.

ErbB-2 and miR-21 are downstream effectors of Stat3-induced BC metastasis

To address ErbB-2 role as downstream mediator of Stat3-induced BC metastasis, we first studied whether Stat3 modulates metastasis in our models. Cells from the DN clones in which we observed higher inhibition of Stat3 phosphorylation and from the VECTOR clone were inoculated subcutaneously in BALB/c mice. All mice developed tumors without significant differences in either latency or tumor take (Supplementary Table S1). However, in accordance with Stat3Y705-F inhibitory effects on cell proliferation (Supplementary Figure S2), volumes and growth rates of DN tumors were lower than those of the VECTOR group (Figure 3a and Supplementary Table S1). At day 42, animals bearing DN tumors
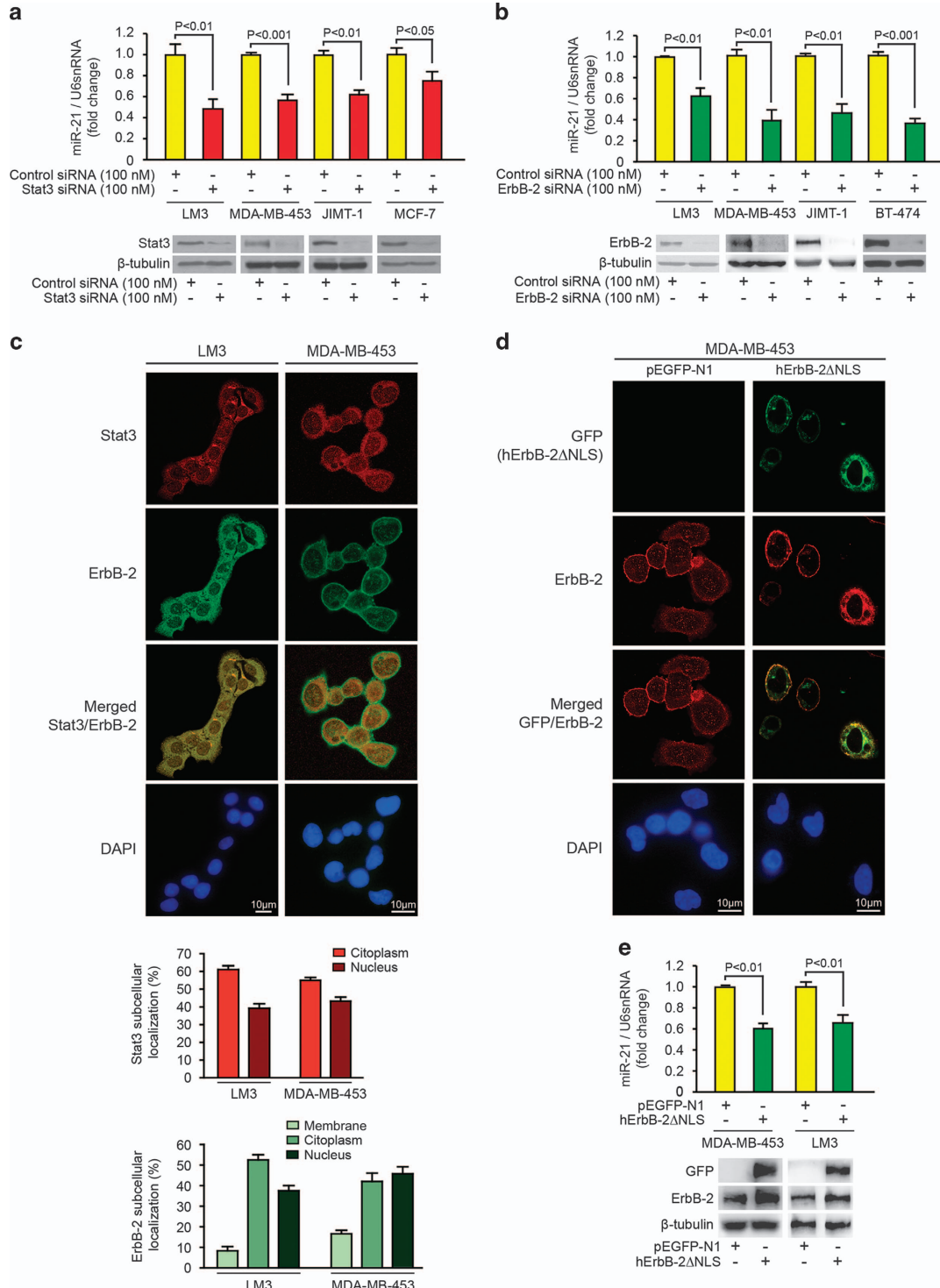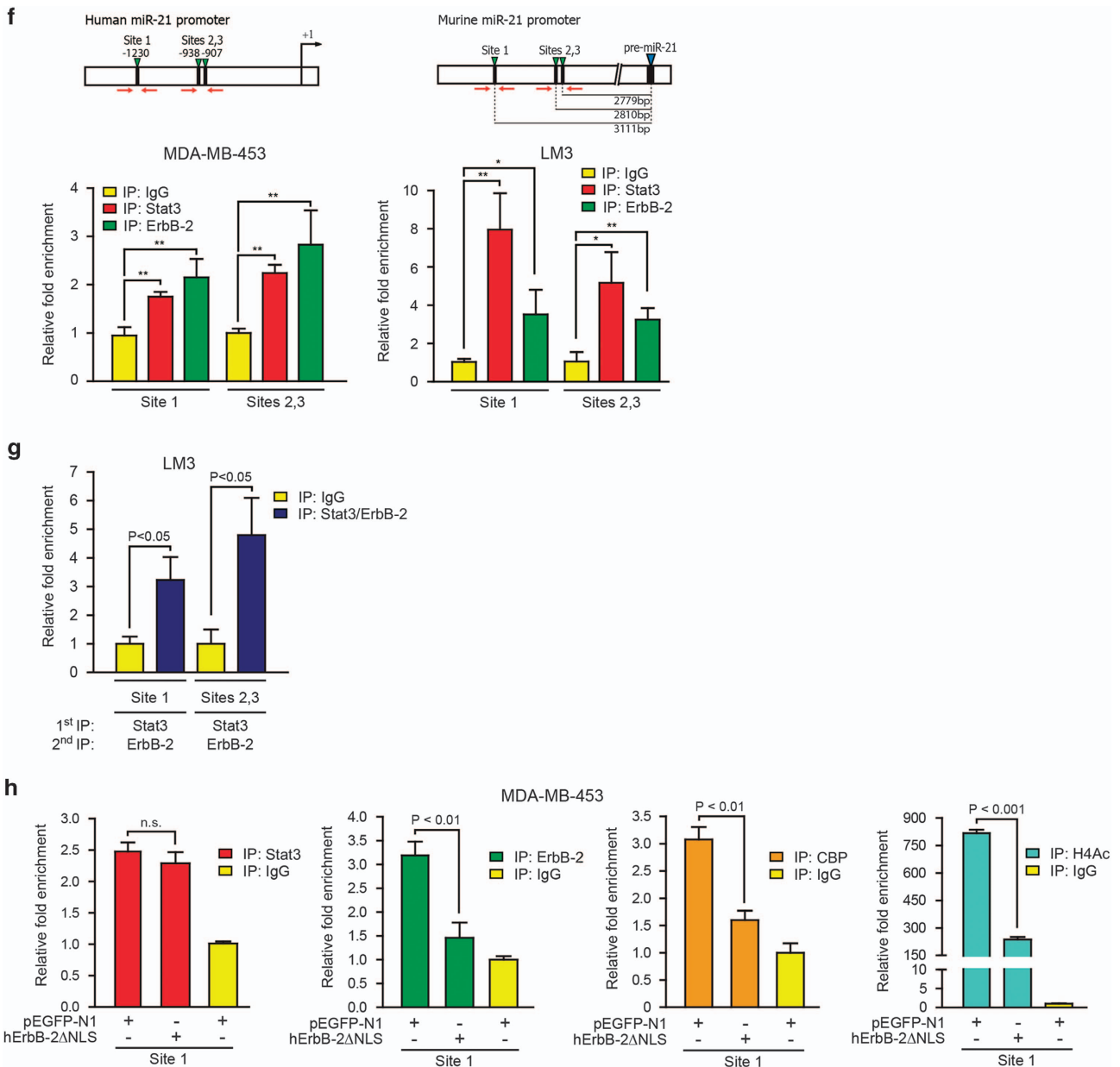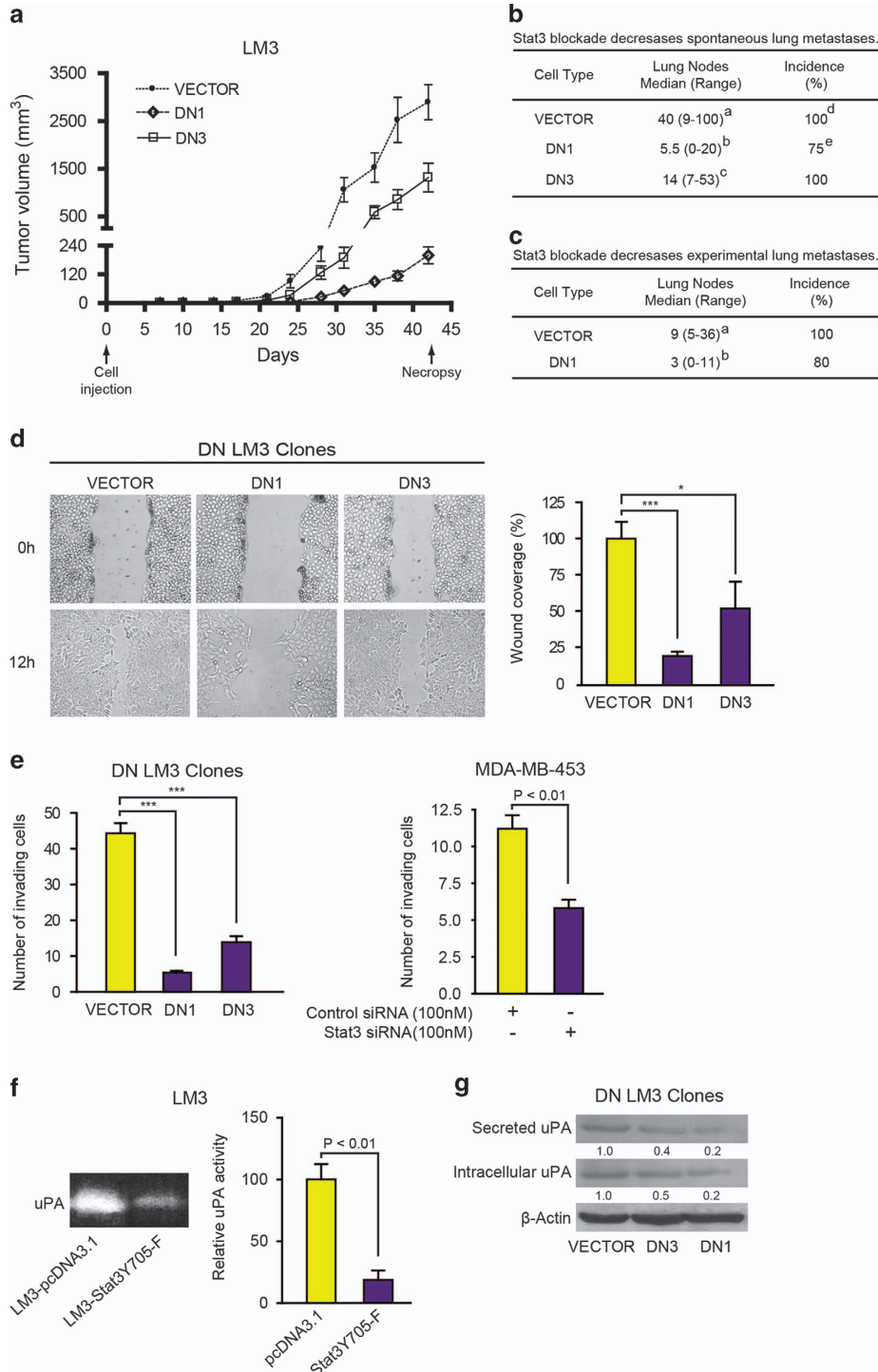

Figure 2. Continued.

Figure 2. Stat3 co-opts ErbB-2 nuclear function to induce miR-21 expression in BC. (**a**) Stat3 silencing reduces miR-21 expression levels. Upper panel: cells were transfected as indicated and miR-21 levels were determined by RT-qPCR. The fold change of miR-21 expression levels was calculated by normalizing the absolute levels of miR-21 to those of U6 snRNA, which was used as internal control, and setting the value of control siRNA-transfected cells to 1. Lower panel: control of inhibition of Stat3 expression by siRNAs. β-tubulin expression was used as loading control. (**b**) ErbB-2 silencing reduces miR-21 expression levels. Upper panel: cells were transfected as indicated and miR-21 levels were determined as in (**a**). Lower panel: control of inhibition of ErbB-2 expression by siRNAs. (**c**) Upper panel: Stat3 (red) and ErbB-2 (green) were localized by immunofluorescence (IF) and confocal microscopy in serum-stimulated LM3 and MDA-MB-453 cells. Merged images show Stat3/ErbB-2 nuclear colocalization in yellow. Nuclei were stained with DAPI (blue). Lower panel: quantitative analysis of Stat3 and ErbB-2 subcellular localization. Red and green fluorescence intensities (integrated intensity per unit area) were quantified in 50 cells from each cell line and are plotted as percentages (mean ± s.d.), relative to the total content (intensity) of Stat3 or ErbB-2 in each cell, which was set to 100%. (**d**) Effect of hErbB-2ΔNLS on ErbB-2 nuclear localization. Cells were transfected with hErbB-2ΔNLS or empty plasmid. GFP from hErbB-2ΔNLS vector was visualized by direct fluorescence imaging (green), and total ErbB-2 (red) was localized by IF and confocal microscopy. Nuclei were stained with DAPI (blue). Images shown in (**a–d**) are representative of three experiments with similar results. (**e**) NErbB-2 is required for miR-21 expression. Upper panel: cells were transfected with hErbB-2ΔNLS and miR-21 levels were determined as in (**a**). Lower panel: content of hErbB-2ΔNLS. WB of GFP and ErbB-2 were performed to confirm transfection. (**f**) Recruitment of Stat3 and ErbB-2 to the miR-21 promoter was analyzed by ChIP. IgG immunoprecipitation was used as a control. Immunoprecipitated DNA was amplified by RT-qPCR using primers (red arrows) flanking the Stat3-binding sites (green arrows) indicated in the upper diagrams. The arbitrary RT-qPCR number obtained for each sample was normalized to the input, setting the value of the IgG samples as 1. $P < 0.05$ for *; $P < 0.01$ for **. (**g**) Stat3 and ErbB-2 are co-recruited to the miR-21 promoter. Chromatins were first immunoprecipitated with a Stat3 antibody and were re-immunoprecipitated using an ErbB-2 antibody. RT-qPCR and data analysis were performed as described above for (**f**). (**h**) Cells were transfected with hErbB-2ΔNLS and recruitment of ErbB-2, Stat3 and CBP, and acetyl-histone H4 levels (H4Ac) at the miR-21 promoter were assessed by ChIP, as stated in (**f**). Data in (**a**, **b**) and (**e–h**) are presented as mean ± s.e.m. of three independent experiments.

showed significantly less incidence and number of spontaneous lung metastases than the VECTOR group (Figure 3b). To demonstrate that decreased metastasis was due to the blockade of Stat3 activation, and not to differences in primary tumor growth, cells from DN1 and VECTOR clones were inoculated into circulation in BALB/c mice to perform an experimental metastasis assay.[44,45] We observed a significant reduction in the incidence and number of lung metastases developed from DN1 clone as compared with VECTOR group (Figure 3c). DN clones also showed decreased migration and invasion than VECTOR cells (Figures 3d and e), and Stat3 knockdown in MDA-MB-453 cells (MDA-MB-453-Stat3-siRNA) reduced their invasion (Figure 3e). Increased expression of proteases is a critical component of the metastasis cascade. We found significantly lower activity of the urokinase-type plasminogen activator (uPA) in the conditioned media of LM3 cells transfected with Stat3Y705-F vector (LM3-Stat3Y705-F) than in parental LM3 cells (Figure 3f). Secreted and intracellular uPA protein levels were lower in DN clones than in VECTOR clone (Figure 3g). These results highlight that Stat3 induces BC metastasis via stimulation of multiple steps of the process.

b Stat3 blockade decresases spontaneous lung metastases.

Cell Type	Lung Nodes Median (Range)	Incidence (%)
VECTOR	40 (9-100)[a]	100[d]
DN1	5.5 (0-20)[b]	75[e]
DN3	14 (7-53)[c]	100

c Stat3 blockade decresases experimental lung metastases.

Cell Type	Lung Nodes Median (Range)	Incidence (%)
VECTOR	9 (5-36)[a]	100
DN1	3 (0-11)[b]	80

Next, we explored the relevance in Stat3-driven BC metastasis of its nuclear interaction with ErbB-2 leading to miR-21 upregulation. LM3 cells in which we silenced Stat3 expression (LM3-Stat3-siRNA), and MDA-MB-453-Stat3-siRNA cells were transfected with a mutant ErbB-2 (V659E), which shows constitutive Tyr kinase activity[46] and induces p42/p44 MAPKs activation when expressed in MCF-7 cells.[47] V659E also migrates to the nucleus of MCF-7 cells (Supplementary Figures S3a and b). Restoration of ErbB-2 levels by transfection of V659E resulted in significantly higher expression of miR-21 than in LM3-Stat3-siRNA and MDA-MB-453-Stat3-siRNA cells (Figure 4a). In spite of the fact that ErbB-2 levels in LM3-Stat3-siRNA and in MDA-MB-453-Stat3-siRNA cells transfected with V659E were comparable to those found in cells with intact Stat3 expression (Figure 4a, lower panels), reconstitution of ErbB-2 expression was unable to upregulate miR-21 expression to the levels in parental cells (Figure 4a). Our finding that ErbB-2 role as Stat3 coactivator regulates miR-21 expression (Figure 2) could explain this inability to fully restore miR-21 levels in the absence of Stat3. On the other hand, the fact that ErbB-2 was found to induce miR-21 via p42/p44 MAPKs[24] might explain the capacity of V659E to partially increase miR-21 in cells lacking Stat3. To further dissect the contribution of NErbB-2 to the expression of miR-21, we transfected LM3-Stat3-siRNA cells with hErbB-2ΔNLS. In spite of the intact role of hErbB-2ΔNLS as an activator of signaling cascades,[12,13,16] miR-21 levels were not upregulated in the absence of NErbB-2 and remained comparable to those in LM3-Stat3-siRNA cells (Figure 4a). These novel findings reveal that, indeed, NErbB-2 function is mandatory for miR-21 upregulation. The difference between V659E and hErbB-2ΔNLS, lies in that V659E migrates to the nucleus and exerts nuclear actions, whereas hErbB-2ΔNLS lacks said capacity.[12] We therefore hypothesize that V659E ability to partially restore miR-21 expression, where Stat3 is not available to assemble Stat3/ErbB-2 complexes, lies on NErbB-2 function as TF. Manual inspection of the human miR-21 promoter revealed the presence of an ErbB-2 binding site (HAS)[17] at position −1193 from the miR-21 transcription start site (37 bp downstream from GAS Site 1). To explore the function of this site, we performed ChIPs using primers flanking GAS Site 1, which also encompass the predicted HAS site. ErbB-2 was strongly loaded to this region in MDA-MB-453 Stat3 siRNA-cells transfected with V659E, even in the absence of Stat3 (Figure 4b). Moreover, CBP loading was detected at this site (Figure 4b). Our reconstitution strategies with ErbB-2 mutants revealed that both ErbB-2 direct role as TF and as a Stat3 coactivator regulate miR-21 expression in metastatic BC cells. To explore the biological significance of these findings, we transfected DN1 clone with V659E. Consistent with ErbB-2 role as a downstream effector of Stat3, V659E expression overcame the inhibition of the invasive capacity caused by the reduction in Stat3

activity (Figure 4c). The role of NErbB-2 in Stat3-regulated metastatic cascade was demonstrated by our finding that transfection of LM3 cells with hErbB-2ΔNLS significantly inhibited migration (Figure 4d). We performed an experimental metastasis assay using LM3-Stat3-siRNA cells, in which we expressed V659E or pre-miR-21. MiR-21 levels achieved by forced pre-miR-21 expression in LM3-Stat3-siRNA cells were comparable to those in LM3 cells with intact Stat3 expression (Figure 4e). As found in the DN1 clone (Figure 3b), LM3-Stat3-siRNA cells showed remarkably lower incidence and number of metastatic lung nodes than the control group (Figure 4f). Transfection with V659E or pre-miR-21 resulted in percentages of incidence and number of lung metastasis comparable to those of the control group (Figure 4f). Histopathological analysis of lung metastatic foci is shown in Supplementary Figure S4a. As the experimental strategy used to abrogate Stat3 expression relied on transient transfections, we explored Stat3 levels in the metastatic foci at the end of the experiment by IF.[12] We found a reduction of ~ 75% in Stat3 levels in metastases from LM3-Stat3-siRNA cells as compared with those from parental cells (Supplementary Figures S4b and c). These findings reveal that ErbB-2 and miR-21 are downstream mediators of Stat3-regulated BC metastasis.
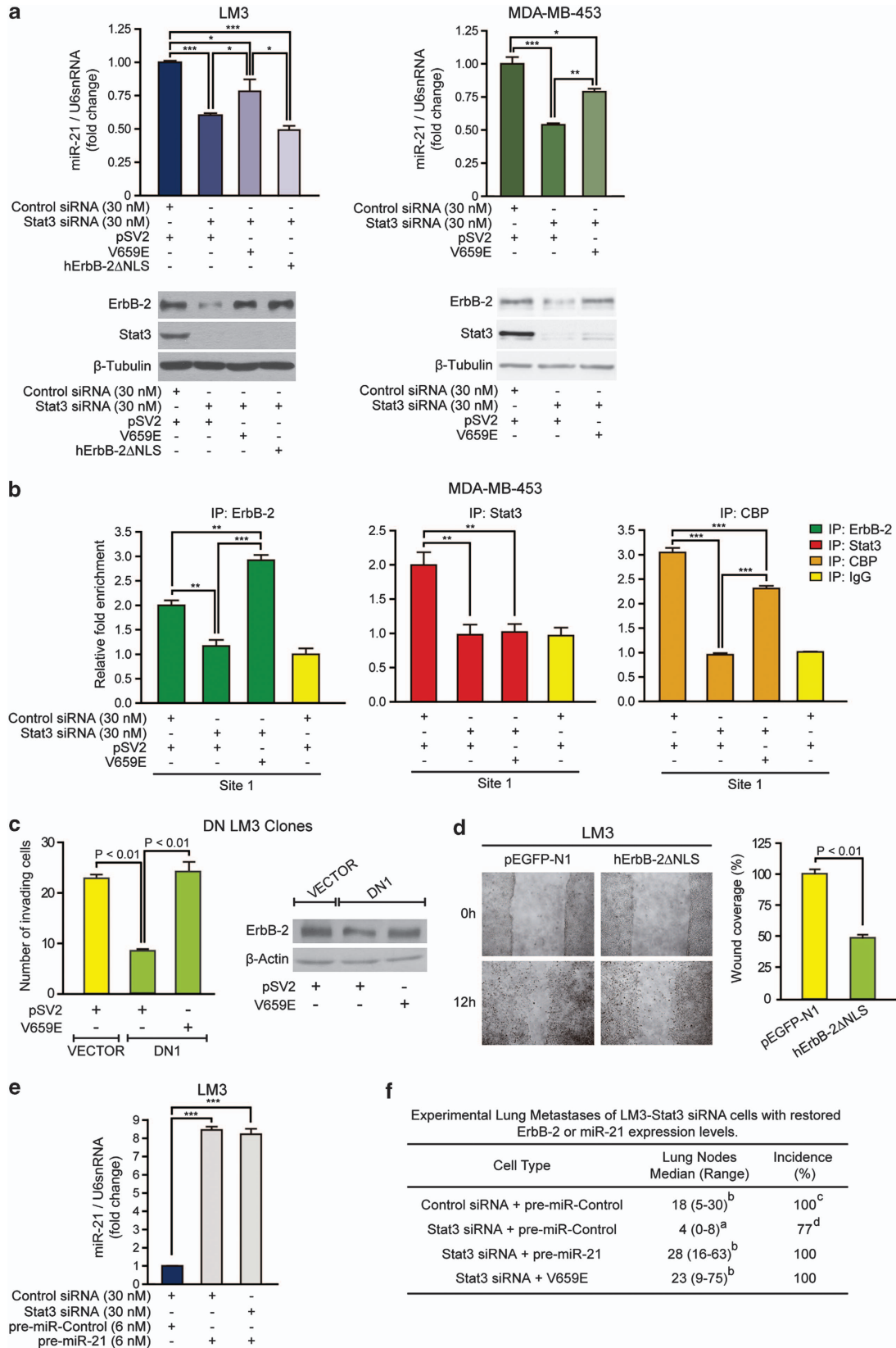
Mir-21 induced by the Stat3/ErbB-2 transcriptional complex downregulates PDCD4

The tumor suppressor gene programmed cell death 4 (PDCD4) is a miR-21 target and its downregulation is involved in miR-21 effects in BC metastasis.[24,28,48,49] We found that miR-21 forced expression induced PDCD4 downregulation in MDA-MB-453 cells (Figure 5a). To study the involvement of the NStat3/NErbB-2 complex on PDCD4 expression, we blocked Stat3 activation, and thus the function of the NStat3/NErbB-2 complex, by transfection with Stat3Y705-F. This strategy also decreases ErbB-2 levels (Figure 1), further compromising the assembly of the complex. Stat3Y705-F strongly upregulated PDCD4 levels (Figure 5b). ErbB-2 silencing, used as a tool to block its signaling and nuclear effects, as well as blockade of NErbB-2 effects by transfection with hErbB-2ΔNLS, also increased PDCD4 content (Figures 5c and d). To further demonstrate NErbB-2 role on PDCD4 levels, mediated via stimulation of miR-21 expression, we took advantage of our previous findings showing that ErbB-2 is not located at the nucleus of serum-starved T47D BC cells (Supplementary Figure S5a and refs. 12, 13). Non-stimulated T47D cells display lower miR-21 levels than those in serum-stimulated LM3 and MDA-MB-453 cells (Figure 5e), which are directly correlated to their respective NErbB-2 levels (Figure 5e displays the quantification of confocal images shown in Supplementary Figure S5a for T47D cells and in Figure 2 for LM3 and MDA-MB-453). Consistently, we found significantly

---

Figure 3. Stat3 activation drives breast cancer tumor growth and metastatic dissemination. (**a**) Preclinical model of *in vivo* blockade of Stat3 activation. Mice were inoculated subcutaneously with cells (3×10^5) from DN or VECTOR clones. Each point represents the mean volume $\pm$ s.e. m. of eight independent tumors from each group. (**b**) Stat3 activation is required for metastatic dissemination. Spontaneous lung metastasis incidence and the number of superficial lung colonies were determined at day 42 and expressed as median and range. $P < 0.001$ for b vs a; $P < 0.05$ for c vs a and for e vs d. (**c**) Mice were inoculated into the tail vein with cells (3×10^5) from DN1 or VECTOR clones. Experimental lung metastasis incidence and the number of superficial lung colonies were determined at day 21 and expressed as in (**b**). $P < 0.05$ for b vs a. (**d**) Blockade of Stat3 activity inhibits migration. Monolayers of DN or VECTOR clones were wounded and allowed to migrate into the cell-free area. Wounded areas were photographed at 0 and 12 h (left) and quantified by densitometry (right). $P < 0.05$ for * and $P < 0.001$ for ***. Experiments shown in (**a**–**d**) were repeated three times with similar results. (**e**) Blockade of Stat3 activity or expression inhibits invasion. VECTOR, DN clones and Stat3 siRNA-transfected MDA-MB-453 cells were seeded in transwell chambers containing full growth media as chemoattractant. After 20 h incubation, cells attached to the lower surface were counted. Data are presented as the average number of invading cells per field $\pm$ s.e.m. $P < 0.001$ for ***. (**f**) Effect of blockade of Stat3 activation on uPA activity. Cells were incubated in serum-free medium for 24 h and uPA activity was evaluated by casein and plasminogen zymography in the supernatant (left). uPA bands underwent densitometry and values were normalized to protein content of the cell monolayer (right). (**g**) uPA secreted protein levels and intracellular protein expression were assessed by WB. Results shown are representative of three independent experiments. Numbers under each blot represent the corresponding densitometric quantification. See Supplementary Figure S2 and Supplementary Table S1.

higher PDCD4 levels in non-stimulated T47D than in LM3 or MDA-MB-453 cells (Figure 5f). HRG treatment of T47D cells, which induces ErbB-2 nuclear migration (Supplementary Figure S5a and ref. 13), resulted in a strong increase in miR-21 and in 60% reduction of PDCD4 levels (Figure 5g). Inhibition of the assembly of the Stat3/ErbB-2 complex by Stat3 knockdown overcame

Cell Type	Lung Nodes Median (Range)	Incidence (%)
Control siRNA + pre-miR-Control	18 (5-30)[b]	100[c]
Stat3 siRNA + pre-miR-Control	4 (0-8)[a]	77[d]
Stat3 siRNA + pre-miR-21	28 (16-63)[b]	100
Stat3 siRNA + V659E	23 (9-75)[b]	100

HRG-induced downregulation of PDCD4 (Figure 5h). Our findings using several strategies and BC models identify Stat3/ErbB-2 transcriptional complex as an upstream inhibitor of PDCD4 expression in BC.

Inverse correlation between NErbB-2/NStat3 co-expression and PDCD4 expression in ErbB-2-positive BC

To explore the clinical significance of our findings, we conducted a retrospective study in a cohort of 48 ErbB-2-positive primary invasive breast carcinomas whose clinical and pathological characteristics are shown in Supplementary Table S2. MErbB-2, NErbB-2, and NStat3 were studied and scored as we reported.[13,50] The expression of PDCD4, mostly a nuclear protein in BC,[51,52] was studied by immunohistochemistry and scored on a 0 to 3 scale as described in Materials and Methods. Scores of 2+ and 3+ were considered positive (Supplementary Figure S6a). Figure 6a shows representative samples. We found an inverse correlation between NErbB-2/NStat3 co-expression and PDCD4 staining (Figure 6b). Also, lack of PDCD4 expression was correlated with nodal metastasis (Figure 6c). Analysis of PDCD4 expression in lymph nodes matching PDCD4-negative primary tumors revealed that lack of PDCD4 was maintained in the patient's lymph node metastases (Supplementary Figure S6b). Finally, we examined the correlation between miR-21 and PDCD4 mRNA levels in ErbB-2-positive BC samples from The Cancer Genome Atlas (TCGA) and observed an inverse correlation between their expression levels (Figure 6d). As we found in our cohort, low PDCD4 showed a positive correlation with nodal metastasis in the TCGA cohort (Figure 6e).

DISCUSSION

The critical role of Stat3 and MErbB-2 in BC development and metastasis has long been demonstrated (reviewed in Freudenberg et al.[53] and Kamran et al.[10]). More recently, miR-21 was identified as an inducer of BC metastasis (reviewed in Krichevsky and Gabriely[54]). However, the functional interaction between all three players in BC metastasis has so far remained unexplored. Here, we first revealed a novel direction of the Stat3 and ErbB-2 interaction in metastatic, ErbB-2-positive BC, where Stat3, activated downstream of ErbB-2, binds to its GAS sites at the ErbB-2 promoter and upregulates ErbB-2 expression. Second, we showed that Stat3 co-opts NErbB-2 function by recruiting ErbB-2 as its coactivator at the promoter of miR-21. We found that also ErbB-2 direct role as a TF regulates miR-21 expression. MiR-21, in turn, downregulates PDCD4. Our findings in in vitro and in vivo BC models showed that both ErbB-2 and miR-21 are downstream effectors of Stat3-driven metastasis. Figure 6f illustrates our proposed model.

Stat3 modulates multiple steps of the metastatic cascade via control of the expression of genes involved in proliferation, survival, migration, invasion and also in the promotion of angiogenesis (Reviewed in Kamran et al.[10]). Several of the Stat3 effects promoting BC metastasis are exerted upon its activation downstream of ErbB-2.[6,7,9,11] Only one previous study showed that a constitutively activated Stat3 variant binds to the same GAS site of the ErbB-2 promoter we studied here, and increases ErbB-2 protein in MCF-7 cells.[41] No biological function of Stat3 regulation of ErbB-2 expression was explored in said work. Ours is therefore the first demonstration that Stat3 induces metastasis via upregulation of ErbB-2.

BC models where transgenic mice carry ErbB-2 under the control of the mouse mammary tumor virus (MMTV) promoter disclosed the role of ErbB-2 in BC development and metastasis, and the involvement of Stat3 as its downstream effector.[55–58] When transgenic mice, expressing an activated neu oncogene (the rat ortholog of human ErbB-2) under MMTV promoter (MMTV-NIC)[55,59] were crossed with Stat3 conditional knockout mice (Stat3[flx/flx]), it was demonstrated that Stat3[flx/flx] mice showed lower metastasis incidence relative to the parental MMTV-NIC strain.[9] Stat3 disruption did not affect tumor initiation but reduced tumor growth in said model. Contrastingly, another study in which Stat3 was deleted in mice carrying activated neu oncogene under the MMTV promoter (MMTV-neu mice), reported that Stat3 was not required for neu-mediated BC initiation or growth.[6] Constitutively active Stat3 was also found to enhance metastasis in MMTV-neu mice.[7] Our results showed that inhibition of Stat3 activity decreased both tumor growth and metastasis in BC displaying constitutively active endogenous ErbB-2. The fact that neu/ErbB-2 expression in transgenic mice models was driven by a strong viral promoter hampered the study of the TFs and the epigenetic mechanisms controlling endogenous ErbB-2 promoter activation in metastatic BC. Our model, where endogenous Stat3 and ErbB-2 interact, mimics human breast tumors. This allowed us to unravel the bidirectional nature of said interplay in metastasis. ErbB-2 overexpression can occur in the absence of gene amplification, indicating the importance of the dysregulation of the transcriptional control of ErbB-2 expression in BC. However, little is known about the TFs that bind to ErbB-2 promoter/enhancers in BC. ER represses ErbB-2 transcription via an enhancer[60] and Foxp3, which inhibits BC cell growth, binds to and represses the ErbB-2 promoter.[61] Contrastingly, AP-2 binding to the ErbB-2 distal promoter enhances ErbB-2 expression.[62]

The outcome of the feed-forward loop between Stat3 activation and ErbB-2 expression is the assembly of a Stat3/ErbB-2 complex at the miR-21 promoter where Stat3 functions as TF and ErbB-2 as its coactivator to upregulate miR-21. Stat3 has been found to

Figure 4. Reconstitution of ErbB-2 and miR-21 expression restores in vivo metastatic phenotype in BC cells lacking Stat3 activity or expression. (**a**) ErbB-2 expression was reconstituted by transfection of V659E or hErbB-2ΔNLS vectors in Stat3-silenced cells. Upper panel: miR-21 levels were determined as in Figure 2. Lower panel: WB shows efficiency of Stat3 silencing and ErbB-2 reconstitution. $P < 0.05$ for *; $P < 0.01$ for **; and $P < 0.001$ for ***. (**b**) Cells were transfected as in (**a**) and indicated protein recruitment to the miR-21 promoter was analyzed by ChIP. Immunoprecipitated DNA was amplified by RT-qPCR using primers flanking GAS Site 1, shown in Figure 2. Amounts of immunoprecipitated DNA were normalized to inputs and are reported relative to the amount obtained by IgG immunoprecipitation, used as control, which was set to 1. $P < 0.01$ for **; $P < 0.001$ for ***. (**c**, left panel) VECTOR and DN1 clone cells were transfected with V659E vector or the empty plasmid and their invasive capacity was studied as in Figure 3. Right panel: WB was performed to verify ErbB-2 protein reconstitution. (**d**) NErbB-2 is required for cellular migration. Monolayers of confluent cells transfected with hErbB-2ΔNLS or empty vector were wounded and migration was assessed as in Figure 3. (**e**) Cells were co-transfected with Stat3 or control siRNAs and a miR-21 precursor (pre-miR-21). MiR-21 levels were assessed by RT-qPCR. $P < 0.001$ for ***. Data in (**a–e**) are presented as mean ± s.e.m of three independent experiments. (**f**) Experimental metastasis assay. LM3 cells were transfected as indicated in (**a**) or co-transfected with Stat3 siRNA and pre-miR-21, and were then injected into the tail vein of syngeneic mice (3×10^5 cells/mouse). At day 21, metastasis incidence and number of superficial lung colonies were determined and expressed as median and range. Shown is a representative experiment of a total of three, with similar results. $P < 0.05$ for b vs a, and for d vs c. See Supplementary Figures S3 and S4.
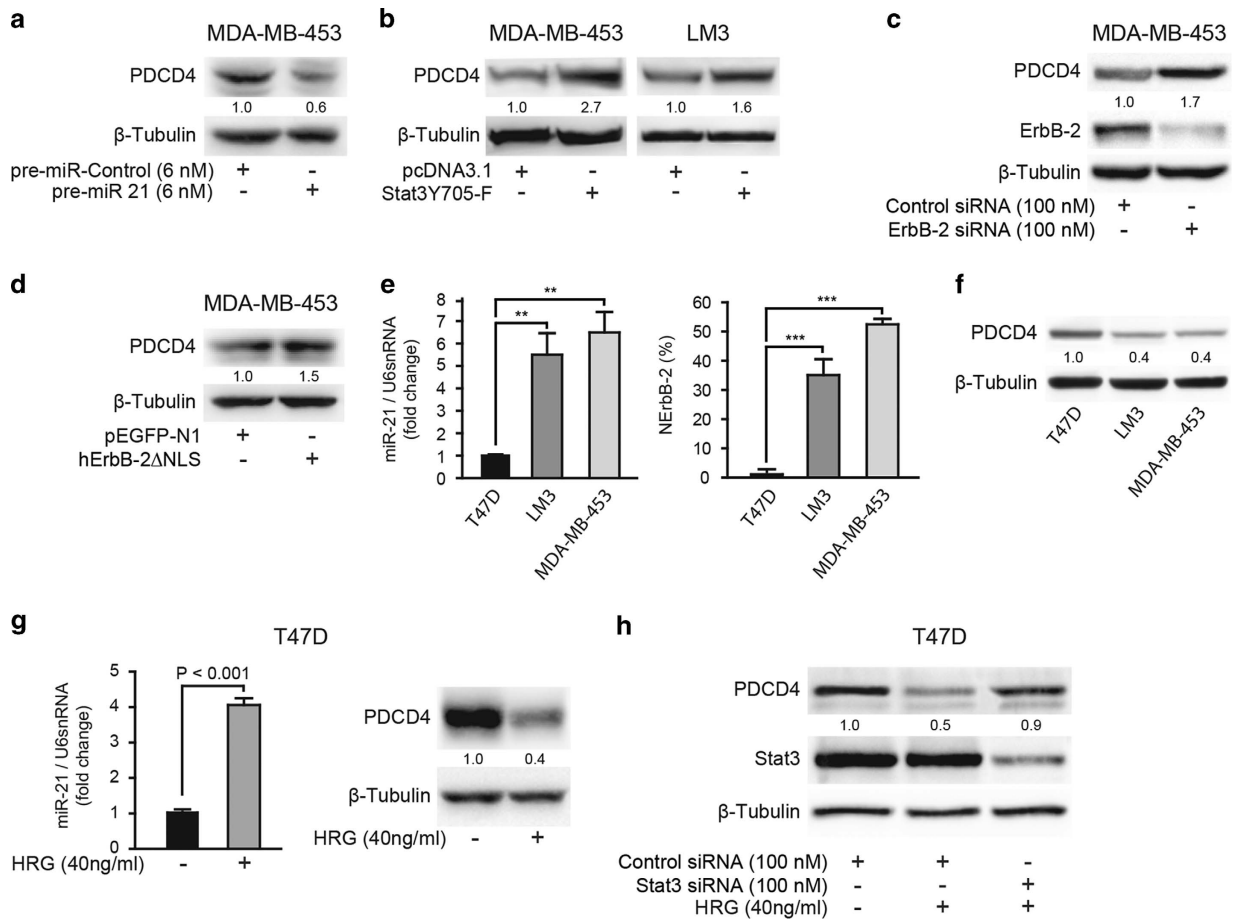
Figure 5. The Stat3/ErbB-2 nuclear complex acts as inhibitor of PDCD4. Cells were transiently transfected with (**a**) pre-miR-21, (**b**) Stat3Y705-F, (**c**) an ErbB-2 siRNA or (**d**) hErbB-2ΔNLS, and PDCD4 levels were assessed by WB. In (**a–d**) experiments shown were repeated three times with similar results. Numbers under each blot represent the corresponding densitometric quantification. (**e**) T47D cells were serum-starved and MDA-MB-453 and LM3 cells were serum-stimulated. Left panel: miR-21 expression levels were studied by RT-qPCR. The fold change of miR-21 was calculated by normalizing the absolute levels of miR-21 to those of U6 snRNA, used as internal control, and setting the value of T47D cells to 1. Right panel: Fluorescence intensities of MErbB-2 and NErbB-2 were quantified in 50 cells from each cell line and expressed as the percentage of NErbB-2. Data are presented as mean ± s.d. $P < 0.01$ for **; $P < 0.001$ for ***. (**f**) Comparison of PDCD4 expression levels was carried out by WB. (**g**) Cells were treated or not with HRG for 48 h. MiR-21 (left) and PDCD4 (right) expression levels were assessed by RT-qPCR and WB, respectively. (**h**) Cells were transfected as indicated and treated with HRG for 48 h. PDCD4 expression levels were analyzed by WB. Shown is a representative experiment of a total of three, with similar results. See Supplementary Figure S5.

control miR-21 expression in several cancer types.[26–28,63–69] Particularly, Stat3 recruitment to its GAS sites at the miR-21 promoter was previously reported in breast, prostate, hepato-cellular and head and neck carcinomas, as well as in transformed mammary epithelial and myeloma cells.[25–28,63,64] In transformed mammary epithelial cells, it is required to maintain the transformed state[25] and in BC cells, Stat3 binding to miR-21 promoter cooperates with NF-κB to induce invasion.[28] Our new findings revealed that Stat3 function as a TF at the miR-21 promoter drives BC metastasis. It was already demonstrated that ErbB-2 upregulates miR-21 in BC via its downstream-activated signaling pathways.[24] We now show that NErbB-2 role as a Stat3 coactivator, and also its direct role as TF, both upregulate miR-21 in BC. NErbB-2 function has been shown to regulate ribosomal RNA synthesis.[70] Our results provide the first evidence, in any cell type, that NErbB-2 also regulates miRNAs expression. Compelling findings, including our own, demonstrated that NErbB-2 stimulates BC growth, induces resistance to anti-MErbB-2 therapies, and is a prognostic factor of poor clinical outcome in ErbB-2-positive tumors.[12–15,17,50,70] Here, we unraveled that NErbB-2 also drives BC metastasis, consistent with a previous study where inactivation of

COX-2, a direct transcriptional target of NErbB-2, hampered migration of ErbB-2-positive BC cells.[17]

In addition to BC, ErbB-2 gene amplification, mutations, and protein overexpression have been reported in several tumor types, including gastric, gastroesophageal, bladder, cervix, colon, endometrium, germ cell, glioblastoma, head and neck, liver, lung, ovarian, pancreas and salivary duct (reviewed in Yan *et al.*[71]). Accumulating evidence demonstrated that ErbB-2 participates in gastric cancer growth, in which targeting MErbB-2 is an effective therapy.[72] As far as we know, among all these different cancer types, ErbB-2 nuclear presence has been reported in small bowel, esophagus and kidney tumor samples, as well as in ovarian cancer cells and in colorectal cancer cell lines upon stimulation with HRG.[17,73] Although Stat3 is expressed in several of these cancer types, its nuclear co-expression with ErbB-2 has only been described in BC. Our present findings raise the exciting possibility that nuclear Stat3 and ErbB-2 jointly regulation of miR-21 expression may be a common mechanism underlying cancer growth and metastatic spreading.

MiR-21 is upregulated in BC samples, as compared with normal tissue[18] and its effects in BC metastasis are mediated via several

target genes, including PDCD4.[24,48,49] ErbB-2 induction of miR-21 via its downstream signaling was found to downregulate PDCD4 and induce migration of BC cells.[24] Results in our experimental models revealed that miR-21, induced by the nuclear Stat3/ErbB-2 interaction, in turn downregulates PDCD4.

Consistent with our results on the mechanism regulating PDCD4 expression, clinical findings in our ErbB-2-positive BC cohort identified an inverse correlation between NErbB-2/NStat3 co-expression and PDCD4 staining. Furthermore, our analysis of ErbB-2-positive BC samples within the TCGA cohort, for the first time identified an inverse correlation between PDCD4 expression at mRNA level and miR-21. Similar inverse relationship between miR-21 and PDCD4 protein was found in BC samples.[48] Our new findings in ErbB-2-positive samples from our own cohort and from that of the TCGA, also revealed that PDCD4 expression is associated with lymph node metastasis in this BC subtype, as reported in ER-positive BC.[74] Our findings (depicted in Figure 6f) indicate that targeting Stat3 and NErbB-2, in combination with current therapies directed to MErbB-2, may be a promising strategy for ErbB-2-positive BC in the metastatic setting.

MATERIALS AND METHODS

Antibodies and reagents
Antibodies and reagents are listed under Supplementary Materials and methods.

Cell lines and treatments
The LM3 mammary tumor cell line was cultured as described.[35] MDA-MB-453 cells were a gift from DJ Slamon (University of California, Los Angeles, CA, USA). MCF-7, BT-474, MDA-MB-231 and T47D cells were obtained from the American Type Culture Collection (Manassas, VA, USA) and JIMT-1 cells from the German Resource Center for Biological Material (Braunschweig, Germany). Cells were maintained as described[13,75] and were routinely tested for mycoplasma contamination. T47D cells were starved in serum-free medium for 48 h before stimulation with heregulin β1 or medroxiprogesterone acetate.

Western blot and urokinase-type plasminogen activator activity assays
Sodium dodecyl sulfate-polyacrylamide gel electrophoresis and immuno-blots were performed as described.[76] To study the expression of urokinase-type plasminogen activator, conditioned media were concentrated using Centricon spin columns (Amino, Beverly, MA, USA). Zymographic analysis was performed as described.[44]

Plasmids, transient transfections and luciferase assays
Plasmids and siRNAs used in this work are detailed under Supplementary Materials and methods. FuGENE HD transfection reagent (Roche Biochem-icals, Indianapolis, IN, USA) was used for plasmid transfection as described.[12] Transfection of siRNAs was performed for 48 h by using DharmaFECT transfection reagent (Dharmacon, Lafayette, CO, USA). For luciferase assays, cells were co-transfected for 48 h with the ErbB-2 promoter construct, RL-CMV plasmid and Stat3 or control siRNA, using DharmaFECT DUO transfection reagent (Dharmacon). Cells were lysed and luciferase assays were completed as described.[12] For reconstitution experiments, Stat3 or control siRNA and pre-miR-21 or pre-miR-Control (Applied Biosystems, Austin, TX, USA), were co-transfected for 36 h using siPORT NeoFx transfection reagent (Ambion, Austin, TX, USA). hErbB-2ΔNLS, V659E or empty plasmid transfection was then performed for 24 h.

Establishment of Stat3Y705-F expressing clones
LM3 cells were transfected with Stat3Y705-F or pcDNA3.1 vectors as described.[37] A detailed protocol is provided under Supplementary Materials and methods.

Migration and invasion assays
Wound-healing assays were performed as described.[34] The invasive potential of cells was measured using Matrigel-coated invasion chambers (Corning Inc., Corning, NY, USA) following manufacturer's instructions. A detailed protocol is provided under Supplementary Materials and methods.

RNA preparation and real-time quantitative RT-PCR
Total RNA was isolated from cells using the miRVANA PARIS Purification Kit (Ambion). Real-time quantitative PCR (RT-qPCR) was performed as described.[12,77] Primers used are listed in Supplementary Materials and methods.

ChIP and sequential ChIP assays
ChIP and sequential ChIP were performed as described.[12] Primers and antibodies used are listed in Supplementary Materials and methods.

In vivo assays
Experiments were conducted in accordance with the NIH Guide for the Care and Use of Laboratory Animals using 2-month-old virgin female BALB/c mice (Institute of Oncology Angel H Roffo, Buenos Aires, Argentina). Studies were approved by the Institute Roffo Animal Research Committee. Animals were randomly assigned to treatment groups using a parallel groups design. In brief, each mouse from a single group was assigned to receive one treatment using a table of random numbers. Spontaneous lung metastases were investigated after subcutaneous inoculation of 3×10^5 DN1, DN3 or VECTOR cells into syngeneic mice ($n=8$ per group). At day 42, animals were killed and the number of superficial lung colonies was determined for each animal by a researcher blinded to the experimental arm. Latency, tumor volume and growth rate were determined as described.[12] For experimental metastasis assays,[44] 3×10^5 cells from DN1 or VECTOR clones, or transiently transfected LM3 cells, were injected into the tail vein of syngeneic mice ($n=8$ per group). At day 21, mice were killed and the number of superficial lung colonies was counted by a researcher blinded to the experimental arm.
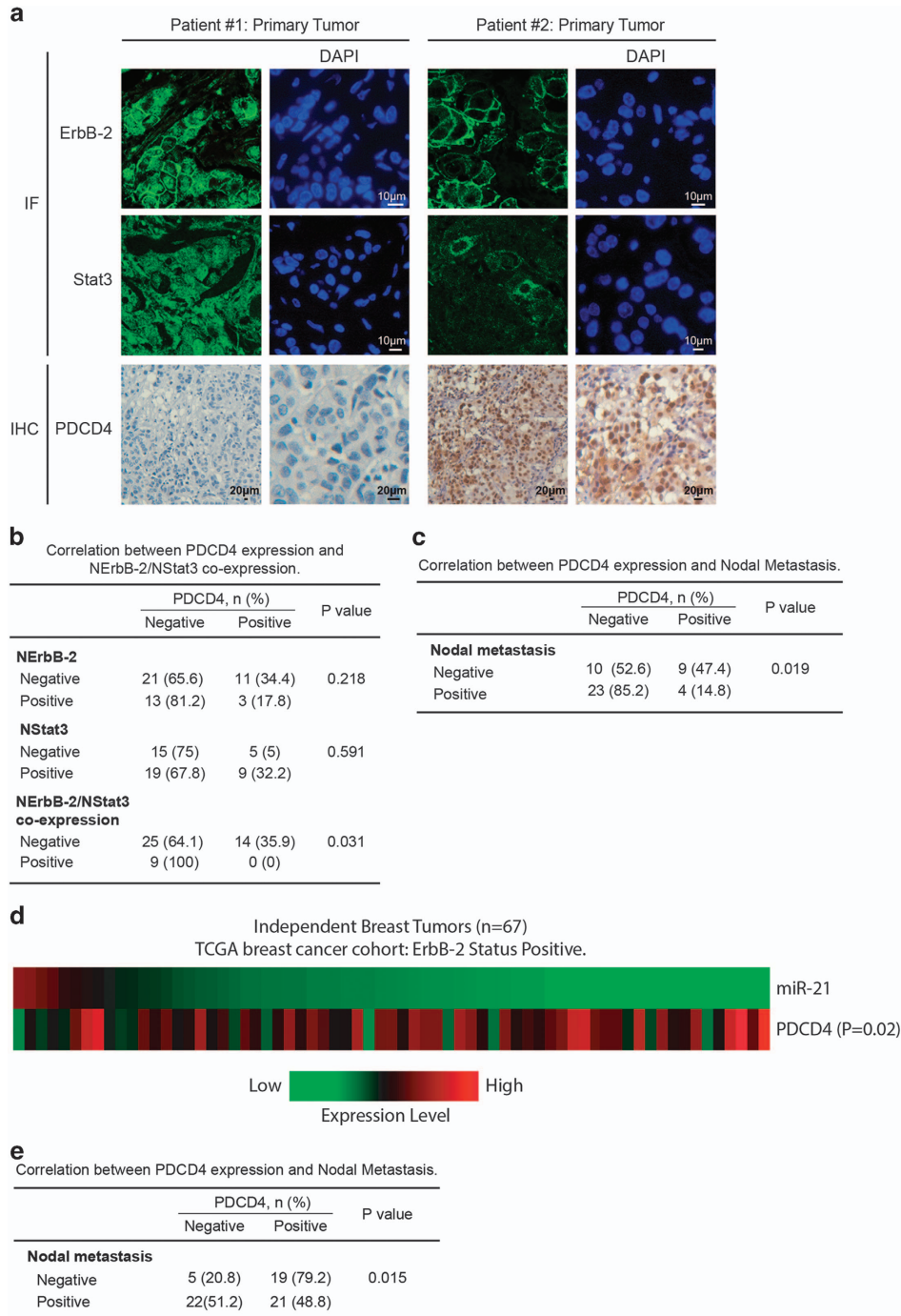
Patients and tissue microarrays
Paraffin-embedded tissue samples from 48 consecutively archived ErbB-2-positive invasive breast carcinomas were selected from the files of the Histopathology Department of Temuco Hospital, Chile. The study was approved by the Institutional Review Board on Human Research of Universidad de La Frontera. Details of informed consents, staging of patients and immunofluorescence analysis are provided in Supplementary Materials and methods.

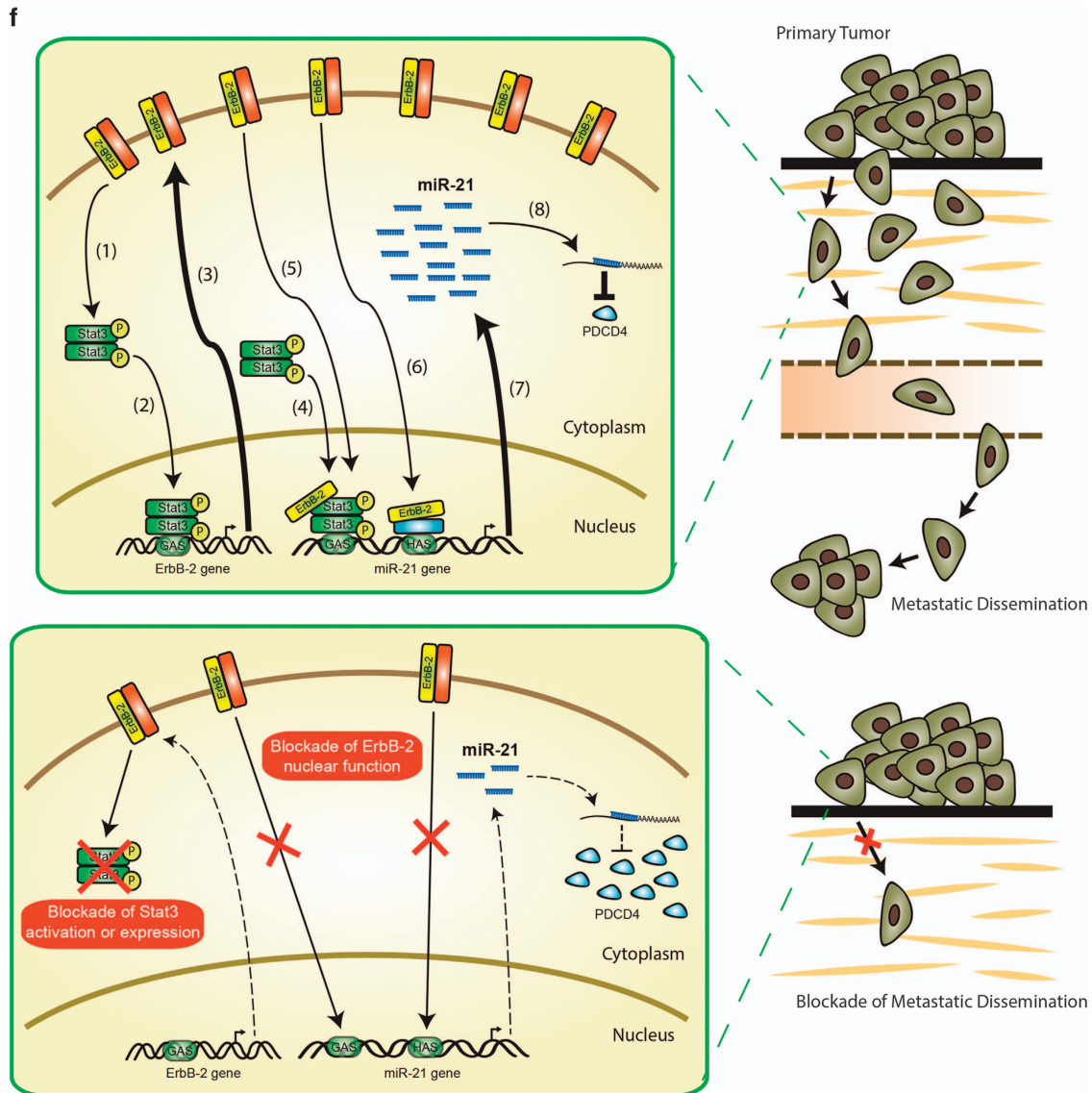### Immunohistochemistry, immunofluorescence and confocal microscopy
Immunohistochemistry was performed as indicated.[77] A description of the quantitative analysis of PDCD4 immunohistochemistry is provided in Supplementary Materials and methods. Immunofluorescence of ErbB-2 and Stat3 in cell cultures and formalin-fixed paraffin-embedded tumors was done as described.[12,13,50] A detailed description of antibodies used and quantitative analysis of confocal images is provided in Supplementary Materials and Methods.

Statistics
When two groups were compared, the two-tailed Student's t-test was used, unless otherwise stated. When three or more groups were compared, homoscedasticity of the variances was analyzed and the one-way analysis of variance test was used, followed by Tukey's test to determine significance between groups. No statistical methods were used a priori to pre-determine sample sizes, but sample sizes were in line with those in previous reports.[44,78,79] The comparison of tumor volumes among different groups was done by analysis of variance followed by Tukey's test. Linear regression analysis was performed on tumor growth curves and the slopes were compared by using analysis of variance followed by a parallelism test to evaluate statistical differences. Comparison of the number of lung metastases among groups was done by the nonparametric Kruskal-Wallis or Mann–Whitney tests. Correlations between categorical variables were performed using the χ^2-test, or Fisher's exact test when the number of observations obtained for analysis was small.

a

Patient #1: Primary Tumor   Patient #2: Primary Tumor

IF — ErbB-2, Stat3
IHC — PDCD4

b

Correlation between PDCD4 expression and
NErbB-2/NStat3 co-expression.

	PDCD4, n (%)		P value
	Negative	Positive	
NErbB-2			
Negative	21 (65.6)	11 (34.4)	0.218
Positive	13 (81.2)	3 (17.8)	
NStat3			
Negative	15 (75)	5 (5)	0.591
Positive	19 (67.8)	9 (32.2)	
NErbB-2/NStat3 co-expression			
Negative	25 (64.1)	14 (35.9)	0.031
Positive	9 (100)	0 (0)	

c

Correlation between PDCD4 expression and Nodal Metastasis.

	PDCD4, n (%)		P value
	Negative	Positive	
Nodal metastasis			
Negative	10 (52.6)	9 (47.4)	0.019
Positive	23 (85.2)	4 (14.8)	

d

Independent Breast Tumors (n=67)
TCGA breast cancer cohort: ErbB-2 Status Positive.

miR-21
PDCD4 (P=0.02)

Low   High
Expression Level

e

Correlation between PDCD4 expression and Nodal Metastasis.

	PDCD4, n (%)		P value
	Negative	Positive	
Nodal metastasis			
Negative	5 (20.8)	19 (79.2)	0.015
Positive	22 (51.2)	21 (48.8)	

Figure 6. Inverse correlation between NErbB-2/NStat3 co-expression and PDCD4 expression in ErbB-2-positive breast tumors. (**a**, upper panel) NErbB-2 and NStat3 levels were evaluated by IF and scored as described in Materials and Methods. Shown are representative images for an ErbB-2-positive tumor with positive co-expression of NErbB-2 (Score 3+) and NStat3 (Score 3+) (left) or a tumor with neither NErbB-2 (Score 0) nor NStat3 (Score 1+) expression (right). Nuclei were stained with DAPI (blue). Lower panels show PDCD4 immunohistochemistry results for these patients. (**b**) Correlation between PDCD4 and NErbB-2 and/or NStat3 expression levels in a MErbB-2-positive BC cohort. (**c**) Correlation between PDCD4 expression and nodal metastasis status for the same cohort as in (**b**). In (**b**, **c**) statistical analysis were performed using Fischer´s exact test. (**d**) Heat map visualization of PDCD4 mRNA and miR-21 expression profiles in primary breast tumors from the TCGA BC cohort, selected on the basis of their ErbB-2 status (analysis conducted using Oncomine). The *P*-value revealing significant correlation between PDCD4 and miR-21 expression levels is presented. (**e**) Correlation between PDCD4 expression status and nodal metastasis for the same cohort as in (**d**). (**f**) Model of the hierarchical interaction between Stat3, NErbB-2 and miR-21 governing BC metastasis in ErbB-2- positive BC. ErbB-2-stimulated phosphorylation of Stat3 at Tyr705 (Step 1, ErbB in red represents the other member of the dimer, that is, ErbB-2, ErbB-3 or EGF-R) induces its activation, nuclear translocation and binding to its GAS sites at the ErbB-2 promoter (Step 2), resulting in enhanced ErbB-2 expression (Step 3). Stat3 is also loaded at the miR-21 gene promoter (Step 4), where it recruits ErbB-2 as its coactivator (Step 5). On the other hand, NErbB-2 binds to it HAS sites at the miR-21 gene promoter (Step 6, blue box represents a potential DNA binding transcription cofactor for ErbB-2). Nuclear Stat3/ErbB-2 complex and NErbB-2 induce miR-21 expression (Step 7), which in turn downregulates PDCD4 (Step 8). Lower panel: proposed blockade of Stat3 and of NErbB-2 function as novel strategies to inhibit metastatic progression. See Supplementary Figure S6 and Supplementary Table S2.

Figure 6. Continued.

AUTHOR CONTRIBUTIONS

PVE, LV and RS were responsible for the conception and design of the study. PVE, LV, LR, AJU, MFC, RICR, VS, EBKJ and RS developed methodology. PVE, LV, LR, AJU, MFC, RICR, MFM, GI, MGP, CJP, FI, MCDF, VS, JCR, PG, EBKJ, EHC and RS acquired the data (and also provided animals, acquired and managed patients, provided facilities and so on). PVE, LV, LR, AJU and RS analyzed and interpreted

the data. PVE, LV and RS wrote the manuscript. PVE supervised the study. All authors read and approved the final manuscript.

REFERENCES

1 Henderson IC, Patek AJ. The relationship between prognostic and predictive factors in the management of breast cancer. *Breast Cancer Res Treat* 1998; **52**: 261–288.
2 Ross JS, Slodkowska EA, Symmans WF, Pusztai L, Ravdin PM, Hortobagyi GN. The HER-2 receptor and breast cancer: ten years of targeted anti-HER-2 therapy and personalized medicine. *Oncologist* 2009; **14**: 320–368.
3 Slamon DJ, Godolphin W, Jones LA, Holt JA, Wong SG, Keith DE *et al.* Studies of the HER-2/neu proto-oncogene in human breast and ovarian cancer. *Science* 1989; **244**: 707–712.
4 Tao RH, Maruyama IN. All EGF(ErbB) receptors have preformed homo- and het-erodimeric structures in living cells. *J Cell Sci* 2008; **121**: 3207–3217.
5 Landgraf R. HER2 therapy. HER2 (ERBB2): functional diversity from structurally conserved building blocks. *Breast Cancer Res* 2007; **9**: 202.
6 Barbieri I, Quaglino E, Maritano D, Pannellini T, Riera L, Cavallo F *et al.* Stat3 is required for anchorage-independent growth and metastasis but not for mammary tumor development downstream of the ErbB-2 oncogene. *Mol Carcinog* 2010; **49**: 114–120.

7 Barbieri I, Pensa S, Pannellini T, Quaglino E, Maritano D, Demaria M et al. Constitutively active Stat3 enhances neu-mediated migration and metastasis in mammary tumors via upregulation of Cten. Cancer Res 2010; 70: 2558–2567.

8 Proietti CJ, Rosemblit C, Beguelin W, Rivas MA, Diaz Flaque MC, Charreau EH et al. Activation of Stat3 by heregulin/ErbB-2 through the co-option of progesterone receptor signaling drives breast cancer growth. Mol Cell Biol 2009; 29: 1249–1265.

9 Ranger JJ, Levy DE, Shahalizadeh S, Hallett M, Muller WJ. Identification of a Stat3-dependent transcription regulatory network involved in metastatic progression. Cancer Res 2009; 69: 6823–6830.

10 Kamran MZ, Patil P, Gude RP. Role of STAT3 in cancer metastasis and translational advances. Biomed Res Int 2013; 2013: 421821.

11 Guo W, Pylayeva Y, Pepe A, Yoshioka T, Muller WJ, Inghirami G et al. Beta 4 integrin amplifies ErbB2 signaling to promote mammary tumorigenesis. Cell 2006; 126: 489–502.

12 Beguelin W, Diaz Flaque MC, Proietti CJ, Cayrol F, Rivas MA, Tkach M et al. Progesterone receptor induces ErbB-2 nuclear translocation to promote breast cancer growth via a novel transcriptional effect: ErbB-2 function as a coactivator of Stat3. Mol Cell Biol 2010; 30: 5456–5472.

13 Cordo Russo RI, Béguelin W, Díaz Flaqué MC, Proietti CJ, Venturutti L, Galigniana N et al. Targeting ErbB-2 nuclear localization and function inhibits breast cancer growth and overcomes trastuzumab resistance. Oncogene 2014; 34: 3413–3428.

14 Diaz Flaque MC, Vicario R, Proietti CJ, Izzo F, Schillaci R, Elizalde PV. Progestin drives breast cancer growth by inducing p21(CIP1) expression through the assembly of a transcriptional complex among Stat3, progesterone receptor and ErbB-2. Steroids 2013; 78: 559–567.

15 Diaz Flaque MC, Galigniana NM, Beguelin W, Vicario R, Proietti CJ, Russo RC et al. Progesterone receptor assembly of a transcriptional complex along with activator protein 1, signal transducer and activator of transcription 3 and ErbB-2 governs breast cancer growth and predicts response to endocrine therapy. Breast Cancer Res 2013; 15: R118.

16 Giri DK, Ali-Seyed M, Li LY, Lee DF, Ling P, Bartholomeusz G et al. Endosomal transport of ErbB-2: mechanism for nuclear entry of the cell surface receptor. Mol Cell Biol 2005; 25: 11005–11018.

17 Wang SC, Lien HC, Xia W, Chen IF, Lo HW, Wang Z et al. Binding at and trans-activation of the COX-2 promoter by nuclear tyrosine kinase receptor ErbB-2. Cancer Cell 2004; 6: 251–261.

18 Volinia S, Calin GA, Liu CG, Ambs S, Cimmino A, Petrocca F et al. A microRNA expression signature of human solid tumors defines cancer gene targets. Proc Natl Acad Sci USA 2006; 103: 2257–2261.

19 Tetzlaff MT, Liu A, Xu X, Master SR, Baldwin DA, Tobias JW et al. Differential expression of miRNAs in papillary thyroid carcinoma compared to multinodular goiter using formalin fixed paraffin embedded tissues. Endocr Pathol 2007; 18: 163–173.

20 Tran N, McLean T, Zhang X, Zhao CJ, Thomson JM, O'Brien C et al. MicroRNA expression profiles in head and neck cancer cell lines. Biochem Biophys Res Commun 2007; 358: 12–17.

21 Lui WO, Pourmand N, Patterson BK, Fire A. Patterns of known and novel small RNAs in human cervical cancer. Cancer Res 2007; 67: 6031–6043.

22 Zhang Z, Li Z, Gao C, Chen P, Chen J, Liu W et al. miR-21 plays a pivotal role in gastric cancer pathogenesis and progression. Lab Invest 2008; 88: 1358–1366.

23 Nam EJ, Yoon H, Kim SW, Kim H, Kim YT, Kim JH et al. MicroRNA expression profiles in serous ovarian carcinoma. Clin Cancer Res 2008; 14: 2690–2695.

24 Huang TH, Wu F, Loeb GB, Hsu R, Heidersbach A, Brincat A et al. Up-regulation of miR-21 by HER2/neu signaling promotes cell invasion. J Biol Chem 2009; 284: 18515–18524.

25 Iliopoulos D, Jaeger SA, Hirsch HA, Bulyk ML, Struhl K. STAT3 activation of miR-21 and miR-181b-1 via PTEN and CYLD are part of the epigenetic switch linking inflammation to cancer. Mol Cell 2010; 39: 493–506.

26 Yang CH, Yue J, Fan M, Pfeffer LM. IFN induces miR-21 through a signal transducer and activator of transcription 3-dependent pathway as a suppressive negative feedback on IFN-induced apoptosis. Cancer Res 2010; 70: 8108–8116.

27 Loffler D, Brocke-Heidrich K, Pfeifer G, Stocsits C, Hackermuller J, Kretzschmar AK et al. Interleukin-6 dependent survival of multiple myeloma cells involves the Stat3-mediated induction of microRNA-21 through a highly conserved enhancer. Blood 2007; 110: 1330–1333.

28 Niu J, Shi Y, Tan G, Yang CH, Fan M, Pfeffer LM et al. DNA damage induces NF-kappaB-dependent microRNA-21 up-regulation and promotes breast cancer cell invasion. J Biol Chem 2012; 287: 21783–21795.

29 Han M, Liu M, Wang Y, Mo Z, Bi X, Liu Z et al. Re-expression of miR-21 contributes to migration and invasion by inducing epithelial-mesenchymal transition consistent with cancer stem cell characteristics in MCF-7 cells. Mol Cell Biochem 2012; 363: 427–436.

30 Song B, Wang C, Liu J, Wang X, Lv L, Wei L et al. MicroRNA-21 regulates breast cancer invasion partly by targeting tissue inhibitor of metalloproteinase 3 expression. J Exp Clin Cancer Res 2010; 29: 29.

31 Marino AL, Evangelista AF, Vieira RA, Macedo T, Kerr LM, Abrahao-Machado LF et al. MicroRNA expression as risk biomarker of breast cancer metastasis: a pilot retrospective case-cohort study. BMC Cancer 2014; 14: 739.

32 Yan LX, Huang XF, Shao Q, Huang MY, Deng L, Wu QL et al. MicroRNA miR-21 overexpression in human breast cancer is associated with advanced clinical stage, lymph node metastasis and patient poor prognosis. RNA 2008; 14: 2348–2360.

33 Petrovic N, Mandusic V, Stanojevic B, Lukic S, Todorovic L, Roganovic J et al. The difference in miR-21 expression levels between invasive and non-invasive breast cancers emphasizes its role in breast cancer invasion. Med Oncol 2014; 31: 867.

34 Puricelli L, Proietti CJ, Labriola L, Salatino M, Balana ME, Aguirre GJ et al. Heregulin inhibits proliferation via ERKs and phosphatidyl-inositol 3-kinase activation but regulates urokinase plasminogen activator independently of these pathways in metastatic mammary tumor cells. Int J Cancer 2002; 100: 642–653.

35 Urtreger A, Ladeda V, Puricelli L, Rivelli A, Vidal M, Delustig E et al. Modulation of fibronectin expression and proteolytic activity associated with the invasive and metastatic phenotype in two new murine mammary tumor cell lines. Int J Oncol 1997; 11: 489–496.

36 O'Brien NA, Browne BC, Chow L, Wang Y, Ginther C, Arboleda J et al. Activated phosphoinositide 3-kinase/AKT signaling confers resistance to trastuzumab but not lapatinib. Mol Cancer Ther 2010; 9: 1489–1502.

37 Proietti C, Salatino M, Rosemblit C, Carnevale R, Pecci A, Kornblihtt AR et al. Progestins induce transcriptional activation of signal transducer and activator of transcription 3 (Stat3) via a Jak- and Src-dependent mechanism in breast cancer cells. Mol Cell Biol 2005; 25: 4826–4840.

38 Bromberg JF, Horvath CM, Besser D, Lathem WW, Darnell JE Jr. Stat3 activation is required for cellular transformation by v-src. Mol Cell Biol 1998; 18: 2553–2558.

39 Kaptein A, Paillard V, Saunders M. Dominant negative stat3 mutant inhibits interleukin-6-induced Jak-STAT signal transduction. J Biol Chem 1996; 271: 5961–5964.

40 Holliday DL, Speirs V. Choosing the right cell line for breast cancer research. Breast Cancer Res 2011; 13: 215.

41 Qian L, Chen L, Shi M, Yu M, Jin B, Hu M et al. A novel cis-acting element in Her2 promoter regulated by Stat3 in mammary cancer cells. Biochem Biophys Res Commun 2006; 345: 660–668.

42 Chen J, Wang X. MicroRNA-21 in breast cancer: diagnostic and prognostic potential. Clin Transl Oncol 2014; 16: 225–233.

43 Cai X, Hagedorn CH, Cullen BR. Human microRNAs are processed from capped, polyadenylated transcripts that can also function as mRNAs. RNA 2004; 10: 1957–1966.

44 Carnevale RP, Proietti CJ, Salatino M, Urtreger A, Peluffo G, Edwards DP et al. Progestin effects on breast cancer cell proliferation, proteases activation, and in vivo development of metastatic phenotype all depend on progesterone receptor capacity to activate cytoplasmic signaling pathways. Mol Endocrinol 2007; 21: 1335–1358.

45 Welch DR. Technical considerations for studying cancer metastasis in vivo. Clin Exp Metastasis 1997; 15: 272–306.

46 Akiyama T, Matsuda S, Namba Y, Saito T, Toyoshima K, Yamamoto T. The transforming potential of the c-erbB-2 protein is regulated by its autophosphorylation at the carboxyl-terminal domain. Mol Cell Biol 1991; 11: 833–842.

47 Kang HJ, Yi YW, Hong YB, Kim HJ, Jang YJ, Seong YS et al. HER2 confers drug resistance of human breast cancer cells through activation of NRF2 by direct interaction. Sci Rep 2014; 4: 7201.

48 Zhu S, Wu H, Wu F, Nie D, Sheng S, Mo YY. MicroRNA-21 targets tumor suppressor genes in invasion and metastasis. Cell Res 2008; 18: 350–359.

49 Nieves-Alicea R, Colburn NH, Simeone AM, Tari AM. Programmed cell death 4 inhibits breast cancer cell invasion by increasing tissue inhibitor of metalloproteinases-2 expression. Breast Cancer Res Treat 2009; 114: 203–209.

50 Schillaci R, Guzman P, Cayrol F, Beguelin W, Diaz Flaque MC, Proietti CJ et al. Clinical relevance of ErbB-2/HER2 nuclear expression in breast cancer. BMC Cancer 2012; 12: 74.

51 Bohm M, Sawicka K, Siebrasse JP, Brehmer-Fastnacht A, Peters R, Klempnauer KH. The transformation suppressor protein Pdcd4 shuttles between nucleus and cytoplasm and binds RNA. Oncogene 2003; 22: 4905–4910.

52 Wen YH, Shi X, Chiriboga L, Matahashi S, Yee H, Afonja O. Alterations in the expression of PDCD4 in ductal carcinoma of the breast. Oncol Rep 2007; 18: 1387–1393.

53 Freudenberg JA, Wang Q, Katsumata M, Drebin J, Nagatomo I, Greene MI. The role of HER2 in early breast cancer metastasis and the origins of resistance to HER2-targeted therapies. Exp Mol Pathol 2009; 87: 1–11.

54 Krichevsky AM, Gabriely G. miR-21: a small multi-faceted RNA. J Cell Mol Med 2009; 13: 39–53.

55 Siegel PM, Ryan ED, Cardiff RD, Muller WJ. Elevated expression of activated forms of Neu/ErbB-2 and ErbB-3 are involved in the induction of mammary tumors in transgenic mice: implications for human breast cancer. *EMBO J* 1999; **18**: 2149–2164.

56 Finkle D, Quan ZR, Asghari V, Kloss J, Ghaboosi N, Mai E et al. HER2-targeted therapy reduces incidence and progression of midlife mammary tumors in female murine mammary tumor virus huHER2-transgenic mice. *Clin Cancer Res* 2004; **10**: 2499–2511.

57 Guy CT, Webster MA, Schaller M, Parsons TJ, Cardiff RD, Muller WJ. Expression of the neu protooncogene in the mammary epithelium of transgenic mice induces metastatic disease. *Proc Natl Acad Sci USA* 1992; **89**: 10578–10582.

58 Muller WJ, Sinn E, Pattengale PK, Wallace R, Leder P. Single-step induction of mammary adenocarcinoma in transgenic mice bearing the activated c-neu oncogene. *Cell* 1988; **54**: 105–115.

59 Ursini-Siegel J, Hardy WR, Zuo D, Lam SH, Sanguin-Gendreau V, Cardiff RD et al. ShcA signalling is essential for tumour progression in mouse models of human breast cancer. *EMBO J* 2008; **27**: 910–920.

60 Bates NP, Hurst HC. An intron 1 enhancer element mediates oestrogen-induced suppression of ERBB2 expression. *Oncogene* 1997; **15**: 473–481.

61 Zuo T, Wang L, Morrison C, Chang X, Zhang H, Li W et al. FOXP3 is an X-linked breast cancer suppressor gene and an important repressor of the HER-2/ErbB2 oncogene. *Cell* 2007; **129**: 1275–1286.

62 Delacroix L, Begon D, Chatel G, Jackers P, Winkler R. Distal ERBB2 promoter fragment displays specific transcriptional and nuclear binding activities in ERBB2 overexpressing breast cancer cells. *DNA Cell Biol* 2005; **24**: 582–594.

63 Bourguignon LY, Earle C, Wong G, Spevak CC, Krueger K. Stem cell marker (Nanog) and Stat-3 signaling promote MicroRNA-21 expression and chemoresistance in hyaluronan/CD44-activated head and neck squamous cell carcinoma cells. *Oncogene* 2012; **31**: 149–160.

64 Li CH, Xu F, Chow S, Feng L, Yin D, Ng TB et al. Hepatitis B virus X protein promotes hepatocellular carcinoma transformation through interleukin-6 activation of microRNA-21 expression. *Eur J Cancer* 2014; **50**: 2560–2569.

65 Ou H, Li Y, Kang M. Activation of miR-21 by STAT3 induces proliferation and suppresses apoptosis in nasopharyngeal carcinoma by targeting PTEN gene. *PLoS One* 2014; **9**: e109929.

66 Shishodia G, Verma G, Srivastava Y, Mehrotra R, Das BC, Bharti AC. Deregulation of microRNAs Let-7a and miR-21 mediate aberrant STAT3 signaling during human papillomavirus-induced cervical carcinogenesis: role of E6 oncoprotein. *BMC Cancer* 2014; **14**: 996.

67 Yang CH, Yue J, Pfeffer SR, Handorf CR, Pfeffer LM. MicroRNA miR-21 regulates the metastatic behavior of B16 melanoma cells. *J Biol Chem* 2011; **286**: 39172–39178.

68 Zhang J, Xiao Z, Lai D, Sun J, He C, Chu Z et al. miR-21, miR-17 and miR-19a induced by phosphatase of regenerating liver-3 promote the proliferation and metastasis of colon cancer. *Br J Cancer* 2012; **107**: 352–359.

69 Zhou X, Ren Y, Liu A, Han L, Zhang K, Li S et al. STAT3 inhibitor WP1066 attenuates miRNA-21 to suppress human oral squamous cell carcinoma growth *in vitro* and *in vivo*. *Oncol Rep* 2014; **31**: 2173–2180.

70 Li LY, Chen H, Hsieh YH, Wang YN, Chu HJ, Chen YH et al. Nuclear ErbB2 enhances translation and cell growth by activating transcription of ribosomal RNA genes. *Cancer Res* 2011; **71**: 4269–4279.

71 Yan M, Parker BA, Schwab R, Kurzrock R. HER2 aberrations in cancer: implications for therapy. *Cancer Treat Rev* 2014; **40**: 770–780.

72 Gomez-Martin C, Lopez-Rios F, Aparicio J, Barriuso J, Garcia-Carbonero R, Pazo R et al. A critical review of HER2-positive gastric cancer evaluation and treatment: from trastuzumab, and beyond. *Cancer Lett* 2014; **351**: 30–40.

73 Mitsui K, Yonezawa M, Tatsuguchi A, Shinji S, Gudis K, Tanaka S et al. Localization of phosphorylated ErbB1-4 and heregulin in colorectal cancer. *BMC Cancer* 2014; **14**: 863.

74 Meric-Bernstam F, Chen H, Akcakanat A, Do KA, Lluch A, Hennessy BT et al. Aberrations in translational regulation are associated with poor prognosis in hormone receptor-positive breast cancer. *Breast Cancer Res* 2012; **14**: R138.

75 Balana ME, Labriola L, Salatino M, Movsichoff F, Peters G, Charreau EH et al. Activation of ErbB-2 via a hierarchical interaction between ErbB-2 and type I insulin-like growth factor receptor in mammary tumor cells. *Oncogene* 2001; **20**: 34–47.

76 Izzo F, Mercogliano F, Venturutti L, Tkach M, Inurrigarro G, Schillaci R et al. Progesterone receptor activation downregulates GATA3 by transcriptional repression and increased protein turnover promoting breast tumor growth. *Breast Cancer Res* 2014; **16**: 491.

77 Rivas MA, Venturutti L, Huang YW, Schillaci R, Huang TH, Elizalde PV. Downregulation of the tumor-suppressor miR-16 via progestin-mediated oncogenic signaling contributes to breast cancer development. *Breast Cancer Res* 2012; **14**: R77.

78 Alonso DF, Skilton G, Farias EF, Bal de Kier JE, Gomez DE. Antimetastatic effect of desmopressin in a mouse mammary tumor model. *Breast Cancer Res Treat* 1999; **57**: 271–275.

79 Peters MG, Farias E, Colombo L, Filmus J, Puricelli L, Bal de Kier JE. Inhibition of invasion and metastasis by glypican-3 in a syngeneic breast cancer model. *Breast Cancer Res Treat* 2003; **80**: 221–232.

Supplementary Information accompanies this paper on the Oncogene website (http://www.nature.com/onc)